Mon. Not. R. Astron. Soc. **344,** 823–834 (2003)

# A theoretician's analysis of the supernova data and the limitations in determining the nature of dark energy

T. Padmanabhan★ and T. Roy Choudhury★
*IUCAA, Ganeshkhind, Pune, India 411 007*

Accepted 2003 June 2. Received 2003 April 25; in original form 2003 January 2

**ABSTRACT**

Current cosmological observations show a strong signature of the existence of a dark energy component with negative pressure. The most obvious candidate for this dark energy is the cosmological constant (with the equation of state $w_X = p/\rho = -1$), which, however, raises several theoretical difficulties. This has led to models for a dark energy component that evolves with time. We discuss certain questions related to the determination of the nature of the dark energy component from observations of high-redshift supernovae. The main results of our analysis are as follows. (i) Even if the precise value of $w_X$ is known from observations, it is *not* possible to determine the nature of the unknown dark energy source using only kinematical and geometrical measurements. We have given explicit examples to show that different types of sources can give rise to a given $w_X$. (ii) Although the full data set of supernova observations (which are currently available) strongly rule out models without dark energy, the high- ($z > 0.25$) and low- ($z < 0.25$) redshift data sets, individually, admit decelerating models with zero dark energy. Any possible evolution in the absolute magnitude of the supernovae, if detected, might allow the decelerating models to be consistent with the data. (iii) We have introduced two parameters, which can be obtained entirely from theory, to study the sensitivity of the luminosity distance on $w_X$. Using these two parameters, we have argued that although one can determine the present value of $w_X$ accurately from the data, one cannot constrain the evolution of $w_X$.

**Key words:** supernovae: general – cosmological parameters – cosmology: miscellaneous.

## 1 INTRODUCTION

One of the equations governing the dynamics of a Friedmann universe, $(\ddot{a}/a) = -(4\pi G/3)(\rho + 3p)$, implies that the Universe will accelerate ($\ddot{a} > 0$) if $(\rho + 3p) < 0$. The analysis of high-redshift supernova data (Riess et al. 1998; Perlmutter et al. 1999; Riess 2000) seems to suggest that $\ddot{a}$ is indeed positive thereby requiring $(\rho + 3p) < 0$. This condition requires at least $\rho$ or $p$ to be negative. Cosmologists have not yet become desperate enough to suggest $\rho < 0$; but there was remarkably low resistance in the community to accepting the existence of a constituent with $w \equiv (p/\rho) < -\frac{1}{3}$. This was, to a great extent, facilitated by the fact that cosmologists have long since toyed with the existence of a non-zero cosmological constant with the stress-tensor $T^i_k = \rho_\Lambda \delta^i_k$ corresponding to $w_\Lambda = -1$. In fact, much before the arrival of supernova data on the scene, there were indications that the Universe actually may be populated by an energy density that is very smoothly distributed over large scales. A very clear argument to this effect was given based on the analysis of APM data in 1990 (Efstathiou, Sutherland & Maddox 1990). Later, the first analysis of the *COBE* data in 1992 indicated that the shape of the standard cold dark matter (SCDM) spectrum needs to be modified and the existence of a smoother energy distribution, such as the cosmological constant will be required (Efstathiou, Bond & White 1992; Padmanabhan & Narasimha 1992). An analysis of a host of observations available in 1996 was used to suggest that the data supports the existence of a non-zero cosmological constant (Bagla, Padmanabhan & Narlikar 1996). Given this background, it was not surprising that the cosmologists were not too shocked by the supernova data that became available from 1998 onwards. Currently, there are also other observations, such as those of the age of the Universe, gravitational lensing surveys, etc., which strongly suggest the presence of a positive cosmological constant (see Padmanabhan 2003, for a comprehensive review and references).

There are, however, well-known deep theoretical problems with the existence of a non-zero cosmological constant $\Lambda$ with a magnitude of about $\Lambda\ (G\hbar/c^3) \approx 10^{-123}$. [These are well documented in the literature and will not be discussed here; for a recent review see Padmanabhan (2003)]. This has prompted a host of activity in which one looks for a dark energy component in the Universe

★E-mail: nabhan@iucaa.ernet.in (TP); tirth@iucaa.ernet.in (TRC)

© 2003 RAS

with $w < -1/3$, which is different from a cosmological constant (see Padmanabhan 2003 and references cited therein). If $w_X(a)$ denotes the time-dependent equation of state parameter for an unknown dark energy component in the Universe, then the equation of motion $\mathrm{d}(\rho_X a^3) = w_X \rho_X \, \mathrm{d}a^3$ integrates to give

$$\rho_X(a) = \rho_X(a_0) \exp\left\{-3 \int_{a_0}^{a} \frac{\mathrm{d}a'}{a'}[1 + w_X(a')]\right\}. \quad (1)$$

If $w_X$ is not identically equal to $-1$, then the dark energy density will evolve with time (even if $w_X$ is a constant). This suggests the possibility that the cosmological 'constant' could be time dependent, thereby alleviating some of the difficulties that arise in the case of $w_X = -1$. Several such models (usually based on scalar fields) have been constructed in the literature, all of which generically have a time-dependent $w_X(a)$. The introduction of such an ad hoc, time-dependent *function* into cosmology, of course, takes away much of the credibility; nevertheless, this issue needs to be settled ultimately by observations and not by aesthetics. (If the observations forces us into a solution that is unaesthetic by current standards, we will either conveniently change the standards or live with it!)

In this paper, we discuss certain questions related to the determination of the nature of the dark energy component from observations related to supernova. This issue has been studied in great detail by several groups and our contribution in this paper will border on pedagogy and will present a particular point of view. In the next section we briefly recall and stress some inherent theoretical degeneracies in these analysis. In Section 3 we reanalyse the currently available supernova data in order to focus attention on some key elements. (These results exist in alternate forms in the published literature but we believe our analysis brings out some features clearly.) Based on the lessons learnt in this section, we carry out a similar analysis for possible future supernova observations and point out what can and cannot be achieved. We have intentionally kept the data analysis at a fairly simple level (indicated in the title by 'a theoretician's analysis'). We subscribe to the point of view that any result that cannot be revealed by a simple analysis of data, but arises through a more complex statistical procedure, is inherently suspect and a conclusion as important as the existence of dark energy with $p < 0$ should pass such a test.

## 2 THEORETICAL DEGENERACIES IN THE FRIEDMANN MODEL

We begin by recalling and stressing some inherent limitations that exists in all attempts to probe the Universe through geometrical measures. The assumption of isotropy and homogeneity implies that the large-scale geometry of the Universe can be described by a metric of the form

$$\mathrm{d}s^2 = \mathrm{d}t^2 - a^2(t)\,\mathrm{d}\boldsymbol{x}^2, \quad (2)$$

where $\mathrm{d}\boldsymbol{x}^2$ denotes the line element of the three-dimensional space in comoving coordinates. In any range of time during which $a(t)$ is a monotonic function of $t$, one can use $a$ [or equivalently, redshift $z = (a/a_0)^{-1} - 1$] as a time coordinate. The metric is then

$$\mathrm{d}s^2 = \frac{1}{H^2(a)}\left(\frac{\mathrm{d}a}{a}\right)^2 - a^2\,\mathrm{d}\boldsymbol{x}^2 = \frac{1}{(1+z)^2}\left[\frac{\mathrm{d}z^2}{H^2(z)} - \mathrm{d}\boldsymbol{x}^2\right], \quad (3)$$

where $H(z) = \dot{a}/a$ is the Hubble parameter.

This equation allows us to draw the following conclusion: the only non-trivial metric function in a Friedmann universe is the function $H(z)$ (besides the curvature of the spatial part of the metric). Hence, any kind of observation based on the geometry of space–time, however, complex it may be, will not allow us to determine anything other than this single function $H(z)$. Since Friedmann equations relate $H^2(z)$ to the *total* energy density in the Universe (assuming that the curvature of the spatial part of the metric is known from independent observations or fixed by some theoretical prejudice), the best we can do from any geometrical observation is to determine the total energy density of the Universe at any given $z$. It is not possible to determine the energy densities of individual components from any geometrical observation.

More explicitly, when several non-interacting sources are present in the Universe, the Friedmann equations give

$$H^2(z) = H_0^2\left[\sum_\alpha \Omega_\alpha \exp\left\{3\int_0^z \frac{\mathrm{d}z'}{1+z'}[1+w_\alpha(z')]\right\} + \Omega_k(1+z)^2\right],$$
$$\Omega_k = 1 - \sum_\alpha \Omega_\alpha, \quad (4)$$

where $\Omega_\alpha$ is the density parameter for the $\alpha$th component (such as radiation, matter, a cosmological constant, etc.) and $w_\alpha(z)$ is the corresponding equation of state parameter. For example, non-relativistic matter ($\Omega_m$) has $w_m = 0$, while a non-evolving cosmological constant ($\Omega_\Lambda$) has $w_\Lambda = -1$. From the above equation, it is clear that one needs to know $\Omega_\alpha$ and $w_\alpha(z)$ of the $N-1$ components [along with geometrical measurements giving $H(z)$] in order to determine the contribution of the $N$th component. If we take $\Omega_k = 0$ corresponding to a flat universe, and assume that there is only dust-like matter and dark energy present in the Universe, then we need to know $\Omega_m$ of non-relativistic dust-like matter and $H(z)$ to obtain a handle on $\Omega_X$ of the dark energy. Unfortunately, even after making these assumptions, we are plagued by the uncertainties in $\Omega_m$, which is currently estimated to be anywhere between 0.2 and 0.35. As has been noted several times in the literature (and as we shall emphasize in Section 4), this is a fairly strong degeneracy.

There is another – and from a theoretical point of view more serious – degeneracy that seems to have been inadequately stressed in the literature. Let us assume that the Universe is made of two components: $\rho_{\mathrm{kn}}(a)$, which is known from independent observations and a component $\rho_X(a)$ that is not known. From the Friedmann equation, it follows that

$$\frac{8\pi G}{3}\rho_X(a) = H^2(a)[1 - \Omega_{\mathrm{kn}}(a)]; \quad \Omega_{\mathrm{kn}}(a) \equiv \frac{8\pi G \rho_{\mathrm{kn}}(a)}{3H^2(a)}. \quad (5)$$

Taking a derivative of $\ln \rho_X(a)$ and using (1), it is easy to obtain the relation

$$w_X(a) = -\frac{1}{3}\frac{\mathrm{d}}{\mathrm{d}\ln a}\ln\left\{[1 - \Omega_{\mathrm{kn}}(a)]H^2(a)a^3\right\}. \quad (6)$$

If geometrical observations of the Universe give us $H(a)$ and other observations give us $\rho_{\mathrm{kn}}(a)$ then one can determine $\Omega_{\mathrm{kn}}(a)$ and thus $w_X(a)$. This is the best uniform background cosmology can do for us. As far as cosmological model building is concerned, one is usually interested in the features of the dark energy 'fluid', and it is usually sufficient to know $w_X(a)$ and the speed of sound of the fluid. However, theoretical physicists would like to know something more concerning the nature of the dark energy 'fluid' – in particular, they would find it useful to determine the Lagrangian for the fluid. (For example, in the case of inflation, a considerable amount of effort is being spent on understanding the form of the potential for the scalar field.) In this paper, we shall take the viewpoint of a theoretical physicist, where the nature of the dark energy is defined by its Lagrangian.

Now, if a geometrical observation in future suggest that $w_X(a)$ is not identically equal to $-1$, then the question arises of what is the nature of this dark energy field? It seems virtually impossible that its nature can be determined from laboratory experiments (unlike, for example, WIMPS, which might constitute dark matter). However, knowing $w_X(a)$ is grossly inadequate for determining the physical nature of dark energy. For example, even if one makes another gigantic leap of faith and assumes that the dark energy arises from a scalar field, it is possible to come up with scalar field Lagrangians of different forms leading to the same $w_X(a)$ (see Padmanabhan 2002b). To illustrate this point,we shall discuss two possibilities:

$$L_{\rm quin} = \frac{1}{2}\partial_i\phi\partial^i\phi - V(\phi),$$
$$L_{\rm tach} = -V(\phi)\sqrt{1-\partial_i\phi\partial^i\phi}. \tag{7}$$

Both of these Lagrangians involve one arbitrary function $V(\phi)$. The first one, $L_{\rm quin}$, which is a natural generalization of the Lagrangian for a non-relativistic particle $[L = \dot{q}^2/2 - V(q)]$, is usually called quintessence. Similarly, the second one, $L_{\rm tach}$, is a generalization of the Lagrangian for a relativistic particle $[L = -m\sqrt{1-\dot{q}^2}]$, and is usually called a tachyonic Lagrangian. [It arises naturally in the string theoretical context; see Sen (2002a,b,c). For a discussion of the cosmological aspects of this Lagrangian, see Padmanabhan & Choudhury (2002) and references therein.] When these Lagrangians act as sources in a Friedmann universe, they are characterized by density and equation of state parameters given by

$$\rho_{X,\rm quin} = \frac{1}{2}\dot{\phi}^2 + V, \quad w_{X,\rm quin} = \frac{1-(2V/\dot{\phi}^2)}{1+(2V/\dot{\phi}^2)} \tag{8}$$

and

$$\rho_{X,\rm tach} = V\sqrt{1-\dot{\phi}^2}, \quad w_{X,\rm tach} = \dot{\phi}^2 - 1, \tag{9}$$

respectively.

Since both the Lagrangians have one undetermined function $V(\phi)$, it is possible to choose this function in order to produce a given $w_X(a)$ [or equivalently, $H(a)$]. For a flat universe, one can determine the function $V(\phi)$ for the quintessence model from the implicit relations (Ellis & Madsen 1991)

$$V(a) = \frac{H(a)}{16\pi G}[1-\Omega_{\rm kn}(a)]\left[6H(a) + 2aH'(a) - \frac{aH(a)\Omega'_{\rm kn}(a)}{1-\Omega_{\rm kn}(a)}\right] \tag{10}$$

$$\phi(a) = \left(\frac{1}{8\pi G}\right)^{1/2}\int\frac{{\rm d}a}{a} \times\left\{a\Omega'_{\rm kn}(a) - [1-\Omega_{\rm kn}(a)]\frac{{\rm d}\ln H^2(a)}{{\rm d}\ln a}\right\}^{1/2}. \tag{11}$$

Similarly, in the case of a tachyonic scalar field, the potential function is given by (Padmanabhan 2002b)

$$V(a) = \frac{3H^2(a)}{8\pi G}[1-\Omega_{\rm kn}(a)]\left\{1 + \frac{2}{3}\frac{aH'(a)}{H(a)} - \frac{a\Omega'_{\rm kn}(a)}{3[1-\Omega_{\rm kn}(a)]}\right\}^{1/2} \tag{12}$$

$$\phi(a) = \int\frac{{\rm d}a}{aH(a)}\left\{\frac{a\Omega'_{\rm kn}(a)}{3[1-\Omega_{\rm kn}(a)]} - \frac{2}{3}\frac{aH'(a)}{H(a)}\right\}^{1/2}. \tag{13}$$

We can present an explicit example of a situation where $w_X$ is assumed to be known of the simple form

$$w_X(z) = w_0 - w_1(a-1) = w_0 + w_1\frac{z}{1+z}, \tag{14}$$

where $w_0$ measures the current value of the parameter and $-w_1$ gives its rate of change (with respect to the scalefactor) at the present epoch. In addition to simplicity, this parametrization has the advantage of giving finite $w_X$ in the entire range $0 < z < \infty$. We shall use this simple parametrization later to discuss the possibility of constraining $w_X$ from observations. The Hubble parameter in this case is given by

$$\frac{H^2(z)}{H_0^2} = \Omega_m(1+z)^3 + (1-\Omega_m)(1+z)^{3(1+w_0+w_1)}{\rm e}^{-3w_1 z/(1+z)}. \tag{15}$$

This equation of state parameter can be obtained (for small values of $|w_1|$) from at least two scalar field Lagrangians – those for the quintessence and tachyonic fields. The corresponding potentials $V(\phi)$ can be determined from equations (11) and (12). Unfortunately, the relations cannot be written in a closed form (unless $w_1 = 0$) in this case. The form of the potential for both cases can be calculated numerically for given values of $w_0$ and $w_1$, which are plotted in Fig. 1. The left-hand frame shows $V(\phi)$ for the quintessence field, while the right-hand frame shows that for the tachyonic field. The potentials are plotted for the parameter values $\Omega_m = 0.3$, $\Omega_X = 1 - \Omega_m = 0.7$, $w_0 = 0.5$, $w_1 = -0.1$ using equations (10)–(13). Since the equations give the potential $V(\phi)$ in the parametric form $[V(z), \phi(z)]$, each point on the $V$–$\phi$ curve can be labelled by the corresponding value of redshift, $z$. We have pointed out some particular redshifts in both the curves. It is clear that the scalar field starts from a large value of the potential, rolls down as time progresses and the density contributed by the potential reaches a value $\sim\Omega_X$ at $z = 0$.

This discussion shows that even when $w_X(a)$ or $H(a)$ is known, it is *not* possible to proceed further and determine the nature of the unknown dark energy source using only kinematical and geometrical measurements. This constitutes a serious theoretical problem in cosmology if observations suggest that $w_X$ is not identically equal to $-1$ (Huterer & Turner 1999).

## 3 WARM UP: CURRENT SUPERNOVA DATA AND THEIR ANALYSIS

Next, we shall reanalyse the currently available supernova data in order to stress certain features that are inherent in such an analysis. This may be considered a warm up exercise for the next section.

The observations directly measure the apparent magnitude $m$ of a supernova and its redshift $z$. The apparent magnitude $m$ is related to the luminosity distance $d_L$ of the supernova through

$$m(z) = M + 5\log_{10}\left[\frac{d_L(z)}{1{\rm Mpc}}\right] + 25, \tag{16}$$

where $M$ is the absolute magnitude (which is believed to be constant for all supernovae of Type Ia – this is what is called the 'standard candle hypothesis'). It is convenient to work with a dimensionless quantity (called the 'Hubble-constant-free' luminosity distance)

$$Q(z) \equiv \frac{H_0}{c}d_L(z), \tag{17}$$

which gives

$$m(z) = \mathcal{M} + 5\log_{10}Q(z), \tag{18}$$

where

$$\mathcal{M} = M + 5\log_{10}\left(\frac{c/H_0}{1{\rm Mpc}}\right) + 25 = M - 5\log_{10}h + 42.38. \tag{19}$$

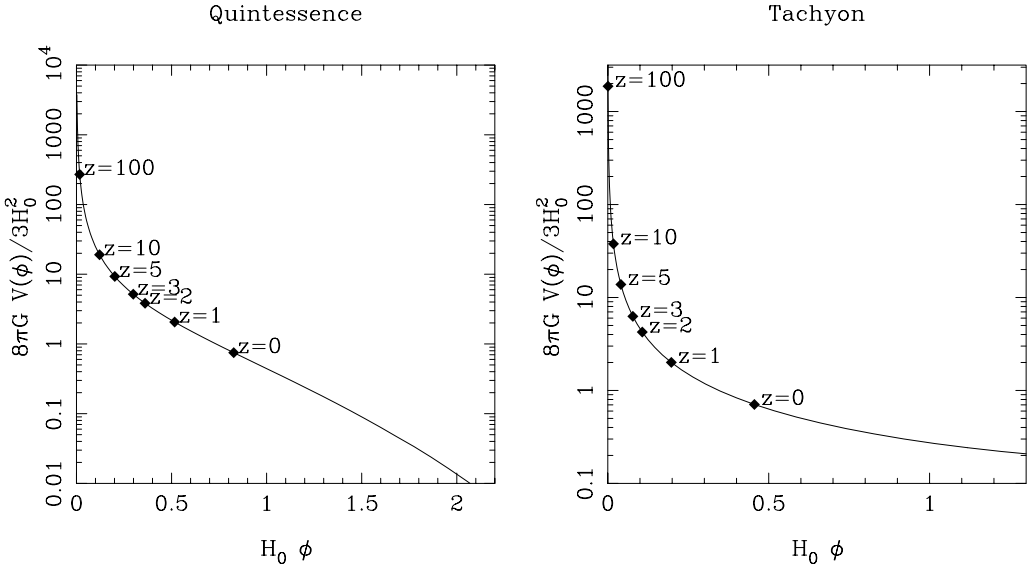


**Figure 1.** The scalar field potentials for the quintessence (left-hand frame) and tachyonic (right-hand frame) fields, which are required to produce the dark energy equation of state $w_X(a) = w_0 - w_1(a-1)$. The potentials are plotted for the parameter values $\Omega_m = 0.3$, $\Omega_X = 1 - \Omega_m = 0.7$, $w_0 = 0.5$, $w_1 = -0.1$ using equations (10)–(13). Since the equations give the potential $V(\phi)$ in the parametric form $[V(z), \phi(z)]$, each point on the $V$–$\phi$ curve can be labelled by the corresponding value of redshift, $z$. We have pointed out some particular redshifts on both the curves. It is clear that the scalar field starts from a large value of the potential, rolls down as time progresses and the density contributed by the potential reaches a value $\sim\Omega_X$ at $z = 0$.

Any model of cosmology will predict $Q(z)$ with some undetermined parameters (say, for example, $\Omega_m$, $\Omega_\Lambda$). These parameters, along with $\mathcal{M}$ (which is itself a combination of the absolute magnitude of the Type Ia supernova and the Hubble constant), are obtained by comparing with observations. According to the standard hot big bang model of cosmology (see, e.g., Padmanabhan 2002a),

$$Q(z) = (1+z)\frac{\sinh[x(z)\sqrt{\Omega_k}]}{\sqrt{\Omega_k}}, \tag{20}$$

where

$$x(z) = \int_0^z \mathrm{d}z' \frac{H_0}{H(z')}. \tag{21}$$

The data in this paper is based on the redshift–magnitude relation of 54 Type Ia supernovae [excluding six outliers from the full sample of 60, which consists of 18 low-redshift points from the Calán/Tololo supernova survey (Hamuy et al. 1996) and 42 points from the Supernova Cosmology Project (Perlmutter et al. 1999)] and that of supernova 1997ff at $z = 1.755$ (Riess et al. 2001). The values of $m$ used have already been corrected for the supernova light curve width–luminosity relation, galactic extinction and possible $K$-correction. In addition, the magnitude for supernova 1997ff has been corrected for lensing effects (Benítez et al. 2002). Given a cosmological model with some free parameters, we have obtained the best-fitting parameter values and the corresponding covariance matrix using the Levenberg–Marquardt method (Press et al. 1992). The details of this fitting procedure, although quite well known, are given in Appendix A for completeness.

Let us start with flat models with $\Omega_m + \Omega_\Lambda = 1$, $\Omega_k = 0$, which are currently favoured strongly by cosmic microwave background radiation (CMBR) data (for recent results, see Sievers et al. 2003). The simple analysis mentioned above gives a best-fitting value of $\Omega_m$ (after marginalizing over $\mathcal{M}$) to be $0.31 \pm 0.08$. The best-fitting $\mathcal{M}$ (after marginalizing over $\Omega_m$) is found to be $23.95 \pm 0.05$ (all the errors quoted in this paper are $1\sigma$). The comparison between three flat models and the observational data is shown in Fig. 2. In order to determine $Q(z)$ for the observational data points, we have used equation (18) with the best-fitting value $\mathcal{M} = 23.95$.

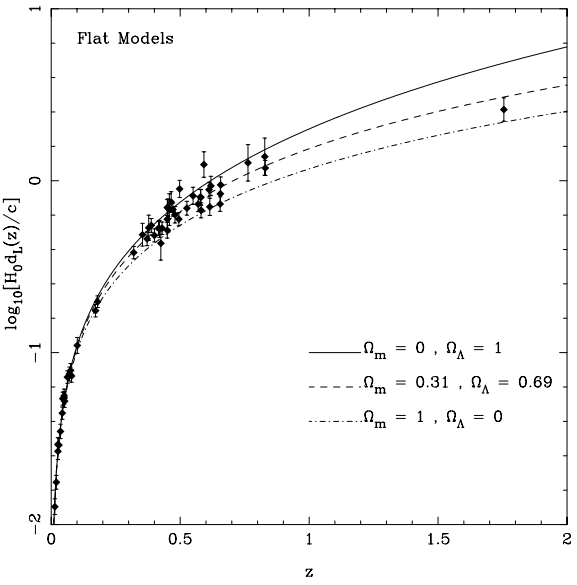


**Figure 2.** A comparison between various flat models and the observational data. The observational data points, shown with error bars, are obtained from Perlmutter et al. (1999) and Riess et al. (2001). In order to determine $Q(z)$ for these data points, we have used equation (18) with the best-fitting value $\mathcal{M} = 23.95$.

Although the best-fitting analysis shows that the data favour strongly for a positive non-zero $\Omega_\Lambda$ which, in turn, implies the presence of an accelerating Universe, the same conclusion is not visually obvious from Fig. 2. In order to see that the data favours models with non-zero $\Omega_\Lambda$, one usually plots the supernova magnitude with respect to a fiducial best-fitting mode (see, for example, Perlmutter et al. 1999) – however, to see the presence of an

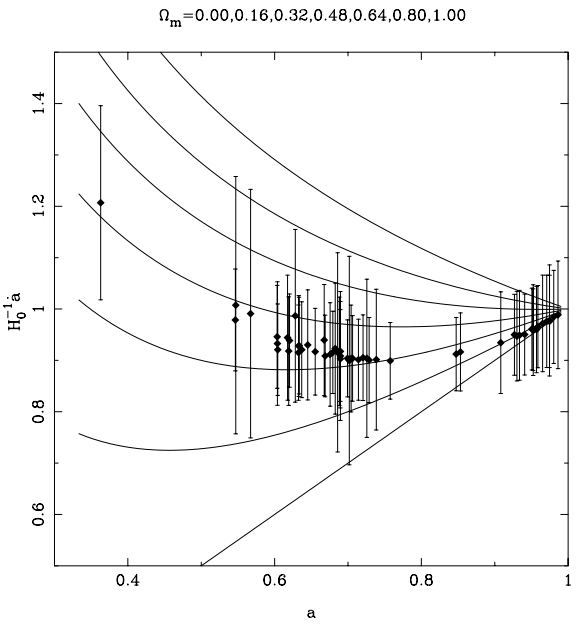


**Figure 3.** The observed supernova data points in the $\dot{a}$–$a$ plane for flat models. The procedure for obtaining the data points and the corresponding error bars are described in the text. The solid curves, from bottom to top, are for flat cosmological models with $\Omega_m = 0.00$, 0.16, 0.32, 0.48, 0.64, 0.80, 1.00, respectively.

accelerating phase, it is more convenient to display the data as the phase portrait of the Universe in the $\dot{a}$–$a$ plane. (The procedure for doing this is described in Appendix B; as far as we are aware, this has not been done in the literature before.) The data points, with error bars, in the $\dot{a}$–$a$ plane are shown in Fig. 3. The solid curves plotted in Fig. 3 correspond to theoretical flat models with different $\Omega_m$.

The data points show a clear sign of an accelerating Universe at low redshifts. Hence, in principle, one should be able to rule out non-accelerating models using only the low-redshift data. However, as is clear from Fig. 3, it is *not* possible to rule out any of the cosmological models using low-redshift ($z \leqslant 0.25$) data because of the large error bars. (The fact that low-redshift data cannot rule out any of the cosmological models can also be seen in Fig. 2.) On the other hand, high-redshift data *alone* cannot be used to establish the existence of a cosmological constant. For example, one can use the freedom in the value of $\mathcal{M}$ to shift the data points vertically, and make them consistent with a decelerating model ($\Omega_m = 1$, topmost curve). It is the interplay between both the high- and low-redshift supernova data that leads to a clear indication of an accelerating phase.

All of the above conclusions can be made more quantitative by studying at the confidence ellipses in the $\Omega_m$–$\mathcal{M}$ plane, shown in Fig. 4. The method of drawing these ellipses is outlined in Appendix A. In the left-hand panel, we have plotted the confidence regions using the full data set of 55 points. It is obvious that most of the probability is concentrated around the best-fitting value. The confidence contours in the middle and right-hand panel are obtained by repeating the best-fitting analysis for the low-redshift data set ($z < 0.25$) and high-redshift data set ($z > 0.25$), respectively. It is clear from the middle panel that, although the low-redshift data can constrain $\mathcal{M}$ very well, it is unable to constrain $\Omega_m$. On the other hand, the high-redshift data (right-hand panel) is able to constrain neither $\mathcal{M}$ nor $\Omega_m$. In particular, the decelerating model ($\Omega_m = 1$) is quite consistent with both the low- and high-redshift data sets when they are treated separately. One needs to combine the low- and high-redshift data to constrain $\Omega_m$ – because of the angular slant of the ellipses, a best-fitting region around $\Omega_m = 0.31$ is isolated, as can be seen from the left-hand panel. [This analysis indirectly stresses the importance of any evolutionary effects. If, for example, supernova at $z \gtrsim 0.25$ and supernova at $z \lesssim 0.25$ have different absolute luminosities because of some unknown effect, then the entire data set can be made consistent with an $\Omega_{\rm m} = 1$, $\Omega_\Lambda = 0$ model. It certainly appears ad hoc; but one should compare the ad-hocness in any of these assumptions with the ad-hocness in introducing a dimensionless constant $\Lambda(G\hbar/c^3) \approx 10^{-123}$ in the physical system to explain the cosmological observations (Padmanabhan 2003)!]

We now generalize some of the results for non-flat cosmologies. In this case, we have three free parameters, namely, $\Omega_m$, $\Omega_\Lambda$ and $\mathcal{M}$. The confidence region ellipses in the $\Omega_m$–$\Omega_\Lambda$ plane can be drawn in two ways: (i) by keeping $\mathcal{M}$ as a free parameter and then marginalizing the joint probability distribution over $\mathcal{M}$ or, (ii) by fixing $\mathcal{M}$ to some constant value (and dealing with only two free parameters, $\Omega_m$ and $\Omega_\Lambda$).

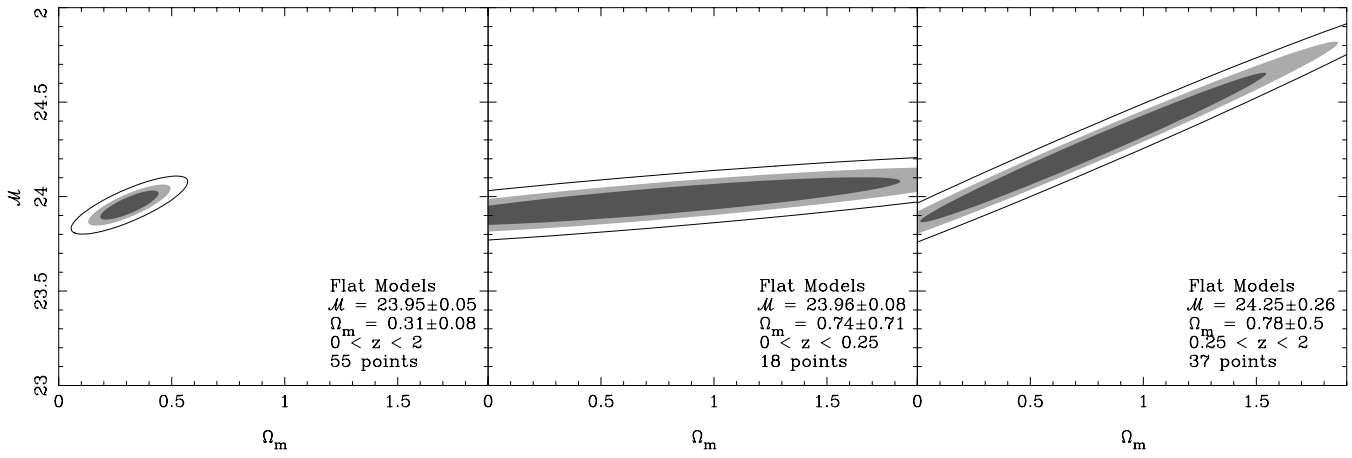


**Figure 4.** Confidence region ellipses in the $\Omega_m$–$\mathcal{M}$ plane for flat models with non-relativistic matter and a cosmological constant. The ellipses corresponding to the 68, 90 and 99 per cent confidence regions are shown. In the left-hand panel, all the 55 data points from Perlmutter et al. (1999) and Riess et al. (2001) are used. In the middle panel, data points with $z < 0.25$ are used, while in the right-hand panel, we have used data points with $z > 0.25$. We have indicated the best-fitting values of $\Omega_m$ and $\mathcal{M}$ (with $1\sigma$ errors). This figure is available in colour in the online version of the journal on *Synergy*.

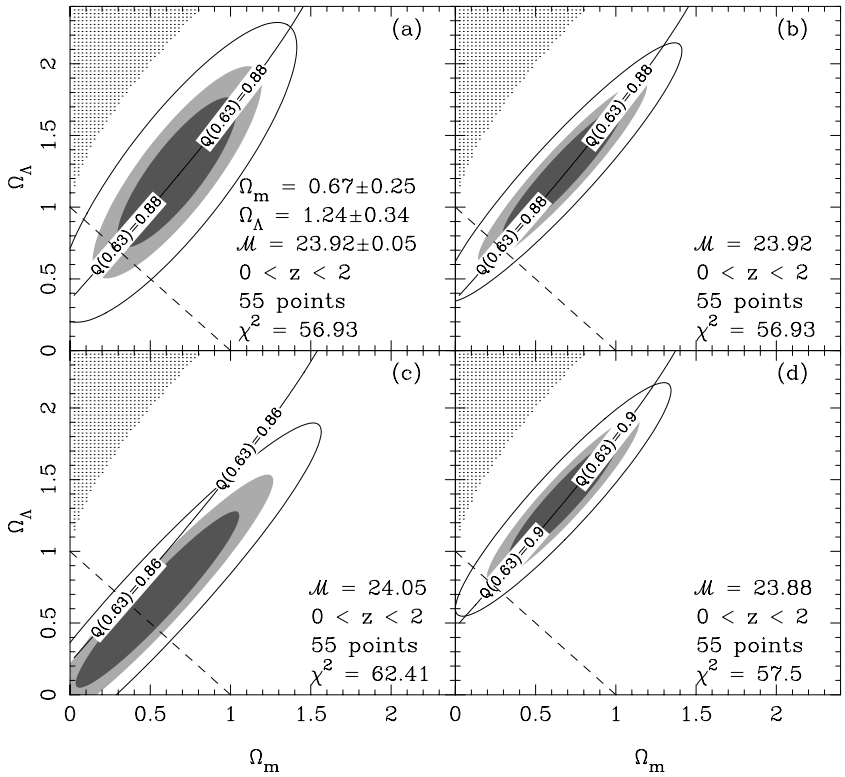


**Figure 5.** Confidence region ellipses in the $\Omega_m$–$\Omega_\Lambda$ plane for models with non-relativistic matter and a cosmological constant. The ellipses corresponding to the 68, 90 and 99 per cent confidence regions are shown. (a) The confidence regions are obtained after marginalizing over $\mathcal{M}$. The best-fitting values of $\Omega_m$ and $\mathcal{M}$ are indicated (with $1\sigma$ errors). (b)–(d) The confidence regions are obtained after fixing $\mathcal{M}$ to its best-fitting mean value and the to the values in the wings of $1\sigma$ limit, respectively. The fixed value of $\mathcal{M}$ is indicated in the panel. The dashed line corresponds to the flat model ($\Omega_m + \Omega_\Lambda = 1$). We have indicated the value of $\chi^2$ for the best-fitting parameters in all the panels. The unbroken slanted line corresponds to the contour of constant luminosity distance, $Q(z = 0.63) =$ constant. This figure is available in colour in the online version of the journal on *Synergy*.

The confidence region ellipses in the $\Omega_m$–$\Omega_\Lambda$ plane are shown in Fig. 5 for the full data set. In panel (a) the confidence regions are obtained by marginalizing over $\mathcal{M}$. The best-fitting values are found to be $\Omega_m = 0.67 \pm 0.25$, $\Omega_\Lambda = 1.24 \pm 0.34$ and $\mathcal{M} = 23.92 \pm 0.05$, as indicated in the panel. For panels (b)–(d), the confidence contours are obtained by fixing $\mathcal{M}$ to a constant value rather than marginalizing over this parameter. The three frames correspond to the best-fitting mean value and two values in the wings of $1\sigma$ from the mean, respectively. The fixed value of $\mathcal{M}$ is indicated in the panel.

The main conclusions we can draw from this figure are: (i) The results do not change significantly whether we marginalize over $\mathcal{M}$ or whether we use the best-fitting value. One can see that the best-fitting values of $\Omega_m$ and $\Omega_\Lambda$ do not change at all, it is only the spread that decreases slightly when we fix $\mathcal{M}$ to a particular value rather than marginalizing it. The two methods give such similar results because the probability of $\mathcal{M}$ is sharply peaked (the spread is $\sim$1 per cent of the mean value). (ii) The results exclude the SCDM model ($\Omega_m = 1$, $\Omega_\Lambda = 0$) at a high level of significance, taking into account the maximum uncertainty in $\mathcal{M}$. The importance of this exercise will be evident later when we consider high- and low-redshift data points separately. (iii) The slanted shape of the probability ellipses show that a particular linear combination of $\Omega_m$ and $\Omega_\Lambda$ is selected out by these observations (which, in this case, turns out to be $0.82\ \Omega_m - 0.57\ \Omega_\Lambda$). This feature, of course, has nothing to do with supernova data and arises purely because the luminosity distance $Q$ depends strongly on a particular linear combination of $\Omega_m$ and $\Omega_\Lambda$. This point is illustrated by plotting the contour of constant luminosity distance, $Q(z = 0.63) =$ constant. The coincidence of this line (which roughly corresponds to $Q$ at a redshift in the middle of the data) with the probability ellipses indicates that it is the dependence of the luminosity distance on cosmological parameters that essentially determines the nature of this result. This fact is known in the literature (see, e.g., Goobar & Perlmutter 1995), but we have not seen the actual data presented in this form. We shall use this result in the next section to discuss the possibility of determining the equation of state parameter for the evolving dark energy component. One should note that a complicated likelihood analysis may give confidence contours of a different shape (they are ellipses only because of the assumption of normal distribution of errors here) – however, the shapes of those contours are bound to show the degeneracy in $\Omega_m$ and $\Omega_\Lambda$ (arising purely from theory) mentioned above. We should also mention that the shapes of the contours of constant $Q$ at high redshifts are quite different from those at low redshifts – hence more high-redshift data can be useful in breaking the degeneracy between $\Omega_m$ and $\Omega_\Lambda$.

As discussed in the third point above, the luminosity distance is sensitive only to a particular linear combination of $\Omega_m$ and $\Omega_\Lambda$, which is illustrated in Fig. 6. In this figure, $\Omega_m$ and $\Omega_\Lambda$ are treated as free parameters (within $2\sigma$ bounds from the best-fitting values mentioned above), but the combination $0.82\Omega_m - 0.57\Omega_\Lambda$ is held fixed. It turns out that $Q(z)$ is not very sensitive to individual values of $\Omega_m$ and $\Omega_\Lambda$ at low redshifts when $0.82\Omega_m - 0.57\Omega_\Lambda$ is in the range $-0.14 \pm 0.11$. This is clear from Fig. 6 in which a wide variety of cosmological models are plotted along with the data for a constant value of the above combination. Though some of the models have

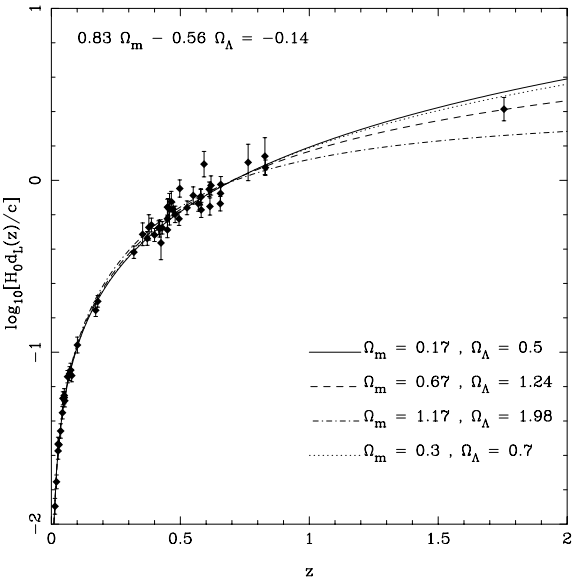


**Figure 6.** The luminosity distance for a class of models with $\Omega_m$ varying between $0.67 \pm 0.50$ and $\Omega_\Lambda$ between $1.24 \pm 0.74$, but with a constant value of the combination $0.82\ \Omega_m - 0.57\ \Omega_\Lambda$. It is clear that when the combination $0.82\ \Omega_m - 0.57\ \Omega_\Lambda$ is fixed, low-redshift observations cannot distinguish between the different models even if $\Omega_m$ and $\Omega_\Lambda$ vary significantly.

unacceptable values of $\Omega_m$ and $\Omega_\Lambda$ (ruled out by observations of CMBR and structure formation), the supernova measurements alone cannot rule them out. Essentially, the data at $z < 1$ are degenerate on the linear combination $0.82\Omega_m - 0.57\Omega_\Lambda$. Our analysis of the supernova data shows that the best-fitting value for this combination is $0.82\Omega_m - 0.57\Omega_\Lambda = -0.14 \pm 0.11$.

Finally, we comment on the interplay between high- and low-redshift data for non-flat models. Just as in the case of the flat models, we divide the full data set into low- ($z < 0.25$) and high- ($z > 0.25$) redshift subsets, and repeated the best-fitting analysis. The resulting confidence contours are shown in Fig. 7. In panel (a), the confidence contours are plotted for the high-redshift data set after marginalizing over $\mathcal{M}$. As we stressed before, the SCDM model cannot be ruled out using high-redshift data alone. In panels (b)–(d), we show the corresponding results in which the values of $\mathcal{M}$ are fixed (rather than marginalizing over $\mathcal{M}$). Comparing Figs 7(a)–(d) with Figs 5(a)–(d), where the full data set was used, we can draw the following conclusions. (i) The best-fitting value for $\mathcal{M}$ is now $24.05 \pm 0.38$; the $1\sigma$ error has now gone up by nearly an order of magnitude compared with the case where the full data was used. Because of this spread, the confidence contours are sensitive to the value of $\mathcal{M}$ one uses, unlike the situation where all the data points were used. (ii) Our conclusions will now depend on the exact value of $\mathcal{M}$ used. For the best-fitting mean value and the lower end of $\mathcal{M}$, the high-redshift data can rule out the SCDM model (see frames b

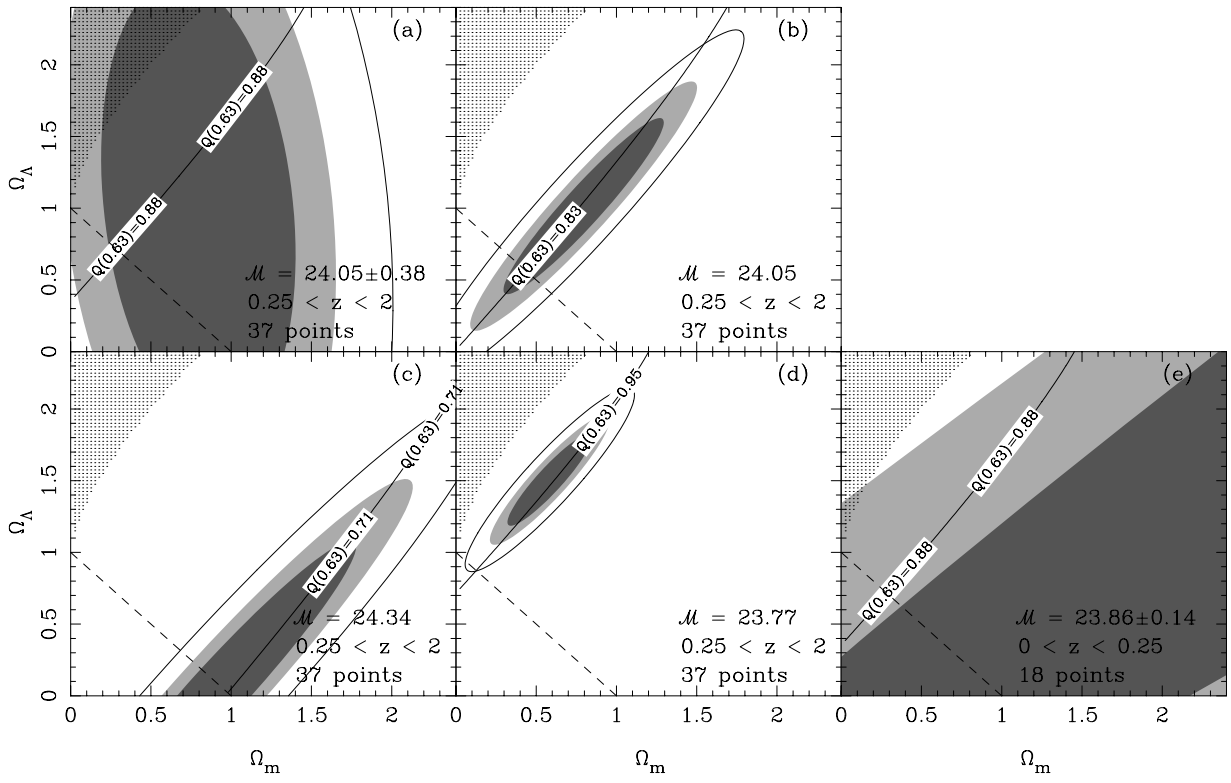


**Figure 7.** Confidence region ellipses in the $\Omega_m$–$\Omega_\Lambda$ plane for models with non-relativistic matter and a cosmological constant. The ellipses corresponding to the 68, 90 and 99 per cent confidence regions are shown. (a) The confidence regions are obtained for high-redshift points ($z > 0.25$), after marginalizing over $\mathcal{M}$. The best-fitting value (with $1\sigma$ error) of $\mathcal{M}$ is indicated. (b)–(d) The confidence regions are obtained for high-redshift points ($z > 0.25$), after fixing $\mathcal{M}$ to its best-fitting value, the upper limit and the lower limit, respectively. The fixed value of $\mathcal{M}$ is indicated in the panel. (e) The confidence regions are obtained for low-redshift points ($z < 0.25$), after marginalizing over $\mathcal{M}$. The best-fitting value (with $1\sigma$ error) of $\mathcal{M}$ is indicated. This figure is available in colour in the online version of the journal on *Synergy*.

and d). However, for the higher end of the allowed $1\sigma$ range of $\mathcal{M}$, we cannot exclude the SCDM model (see c). This essentially shows that it is difficult to rule out models when there are large uncertainties in $\mathcal{M}$. Finally, we plot the contours for the low-redshift data set after marginalizing over $\mathcal{M}$ in panel (e). It is clear that the low-redshift data cannot be used to discriminate between cosmological models effectively. This is because $Q(z)$ at low redshifts is only very weakly dependent on the cosmological parameters. So, even though the acceleration of the Universe is a low-redshift phenomenon, we cannot reliably determine it using low-redshift data alone.

## 4 CONSTRAINTS ON EVOLVING DARK ENERGY

As we have seen in the previous two sections, supernova observations suggest the existence of a non-zero $\Omega_\Lambda$. However, this very existence of $\Omega_\Lambda$ raises serious theoretical problems (see Padmanabhan 2003 for a detailed discussion). These difficulties have led people to consider the possibility that the dark energy is not just a constant – but is evolving with time. The evolution of the dark energy component can be parametrized by its equation of state parameter $w_X(z)$, the evolution of the density $\rho_X$ being given by equation (1). In this section, we shall examine the possibility of constraining $w_X(z)$ by comparing theoretical models with supernova observations.

One simple, phenomenological, procedure for comparing observations with theory is to parametrize the function $w_X(z)$ in some suitable form and to determine a finite set of parameters in this function using the observations. Theoretical models can then be reduced to a finite set of parameters that can be determined from observations. To illustrate this approach, let us assume that, in the flat Universe, $w_X(z)$ is completely determined by its current value ($w_0$) and its rate of change with respect to the scalefactor at the present epoch ($-w_1$) and is given by the simple form as in (14).

Since the cosmological constant corresponds to the case $w_0 = -1$, $w_1 = 0$, it is interesting to see the constraints on $w_0$ from supernova data even if we assume $w_1 = 0$. In such a study, it should be noted that: (i) the acceleration of the Universe requires $w_0 < -\frac{1}{3}$ and (ii) all values of $w_0$ other than $w_0 = -1$ lead to a dark energy density that evolves as $(1+z)^{3(1+w_0)}$. A simple best-fitting analysis shows that for a flat model with $\Omega_m = 0.31$ and $\mathcal{M} = 23.95$ (the best-fitting parameters for flat models, obtained in the previous section), the best-fitting value of $w_0$ is $-1.01 \pm 0.12$ (which is nothing but the conventional cosmological constant). The data clearly rules out models with $w_0 > -\frac{1}{3}$ at a high significance level, thereby supporting the existence of a dark energy component with negative pressure.

One can extend the analysis to find the constraints in the $w_0$–$w_1$ plane. [There is extensive literature on determining dark energy parameters from the current and proposed future supernova observations (e.g. see Maor et al. 2002; Weller & Albrecht 2002; Gerke & Efstathiou 2002 and references therein)]. As before, we assume a flat Universe with a fixed value of $\Omega_m$ in the range (0.21–0.41) and $\mathcal{M}$ is fixed to the corresponding best-fitting value. The confidence contours for the three models are shown in Fig. 8. The square point denotes the equation of state for a universe with a non-evolving dark energy component (the cosmological constant). The main points revealed by this figure are: (i) the equation of state corresponding to the cosmological constant is within the $1\sigma$ contour for $0.21 < \Omega_m < 0.41$. (ii) Despite the uncertainties in $w_1$, models with $w_0 > -1/3$ are ruled out at a high significance level for $\Omega_m < 0.4$. (One can accommodate models with $w_0 > -1/3$ only for $\Omega_m > 0.4$ for very high negative values of $w_1$.) (iii) The shape of the confidence contours clearly indicates that the data are not as sensitive to $w_1$ as compared with $w_0$. Since the supernova observations essentially measure $Q(z)$, this is a clear indication that $Q(z)$ is comparatively insensitive to $w_1$. To see this, note that in Fig. 8, the position of the slanted line [which corresponds to $Q(z = 0.6) =$ constant] exactly coincides with the contour ellipses. We mention again that the shapes of the confidence contours may not remain as simple ellipses if one carries out a complicated likelihood analysis – however, as our conclusions are based on the sensitivity of $Q(z)$ on $w_0$ and $w_1$, they are likely to remain the same for any analysis. Since the determination of $w_0$ and $w_1$ is of considerable importance, we shall provide an illustration of the relative sensitivities of geometrical features to $w_0$ and $w_1$.

As we have stressed in the previous section and also above, the supernova observations essentially measure $Q(z)$, and hence the accuracy in the determination of $w_0$ and $w_1$ from (both present and planned future) supernova observations will crucially depend on

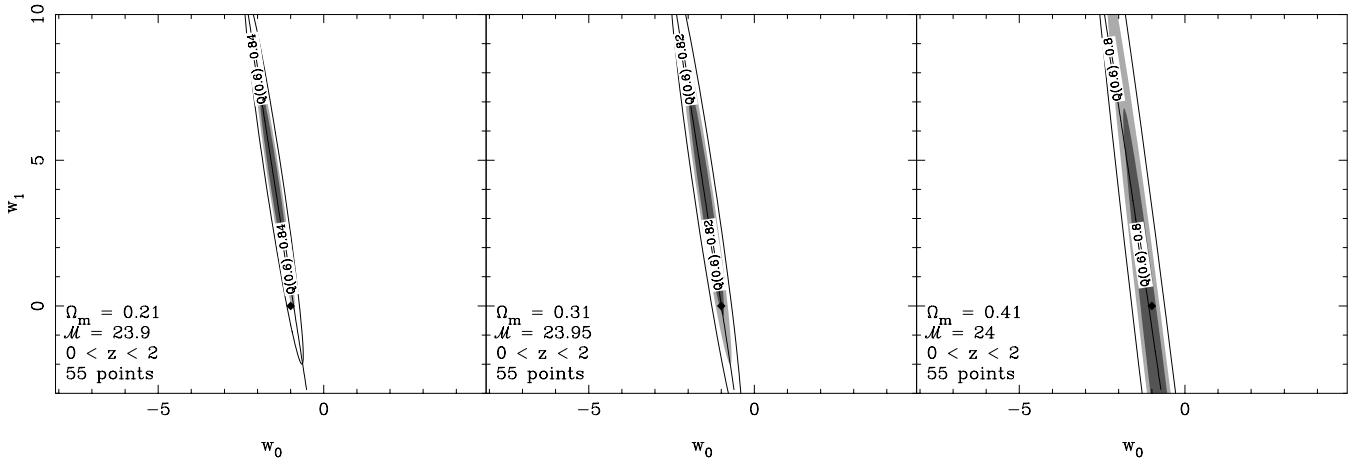


**Figure 8.** Confidence region ellipses in the $w_0$–$w_1$ plane for flat models with $\Omega_m = 0.21$, 0.31 and 0.41, respectively, as indicated in the frames. The value of $\mathcal{M}$ is chosen to be the best-fitting value, which is also indicated. The ellipses corresponding to the 68, 90 and 99 per cent confidence regions are shown. The square point denotes the equation of state for a universe with a non-evolving dark energy component (the cosmological constant). The unbroken slanted line corresponds to the contour of constant luminosity distance, $Q(z = 0.6) =$ constant. This figure is available in colour in the online version of the journal on *Synergy*.

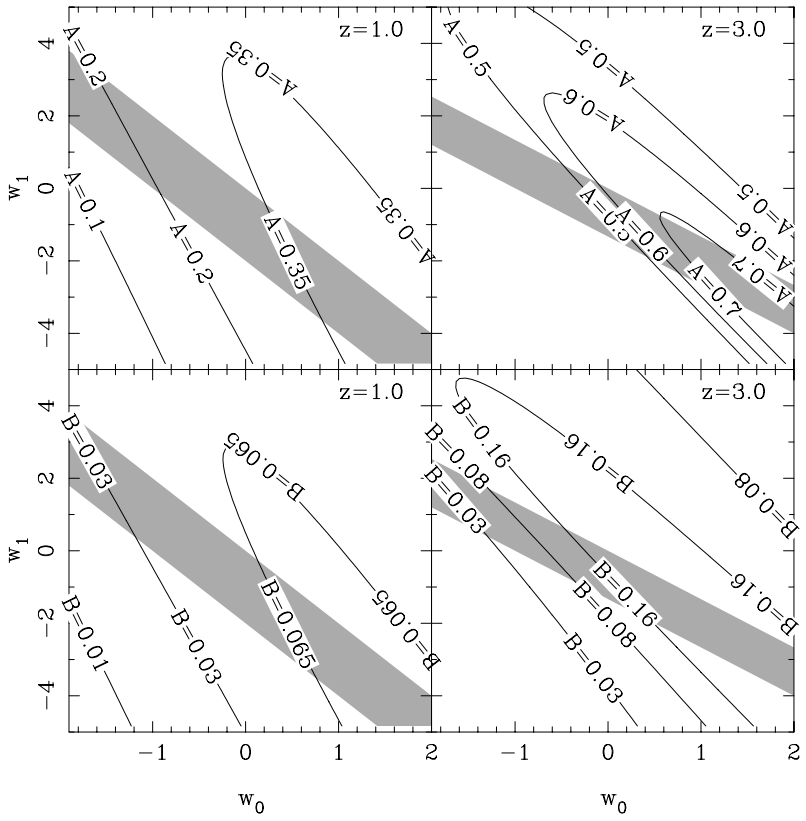


**Figure 9.** Sensitivity of $Q(z)$ to the parameters $w_0$ and $w_1$. The curves correspond to the constant values for the fractional change in $Q$ for unit change in $w_0$ (top frames) and $w_1$ (bottom frames) for two redshifts $z = 1$ (left-hand frames) and $z = 3$ (right-hand frames). The value of $Q$ for a particular curve is indicated. A flat cosmological model with $\Omega_m = 0.31$ has been used. The shaded bands across the frames correspond to the regions in which $-1 \leqslant w_X(z) \leqslant 0$. This figure is available in colour in the online version of the journal on *Synergy*.

how sensitive $Q$ is to the changes in $w_0$ and $w_1$(which is clear from the coincidence of the $Q =$ constant line with the probability ellipses in Fig. 8). A good measure of the sensitivity is provided by the two parameters

$$A(z; w_0, w_1) \equiv \frac{\mathrm{d}}{\mathrm{d}w_0} \ln[Q(z; w_0, w_1)],$$
$$B(z; w_0, w_1) \equiv \frac{\mathrm{d}}{\mathrm{d}w_1} \ln[Q(z; w_0, w_1)]. \tag{22}$$

Like $Q(z; w_0, w_1)$, the parameters $A$ and $B$ can be computed for a particular cosmological model in a straightforward manner. At any given redshift $z$, we can plot contours of constant $A$ and $B$ in the $w_0$–$w_1$ plane. Fig. 9 shows the result of such an analysis for flat models with $\Omega_m = 0.31$. The two frames on the left are for $z = 1$, while those on the right are for $z = 3$. The top frames show the contours of constant $A$, while the bottom frames show the contours of constant $B$. From the definitions (22) it is clear that $A$ and $B$ can be interpreted as the fractional change in $Q$ for unit change in $w_0$ and $w_1$, respectively. For example, along the line marked $A = 0.2$ (in the top left-hand frame), $Q$ will change by 20 per cent for a unit change in $w_0$. It is clear from the two top frames that for most of the interesting region in the $w_0$–$w_1$ plane, changing $w_0$ by unity changes $Q$ by about 10 per cent or more. Comparison of the two cases $z = 1$ and 3 (the two top frames) shows that the sensitivity is higher at high redshift, as is to be expected. The shaded bands across the frames correspond to the regions in which $-1 \leqslant w_X(z) \leqslant 0$, which is of primary interest in constraining dark energy with negative pressure. One concludes from the above discussion that determining $w_0$ from $Q$ fairly accurately will not be too daunting a task.

The situation, however, is quite different for $w_1$ as illustrated in the two bottom frames. For the same region of the $w_0$–$w_1$ plane, $Q$ only changes by a few per cent when $w_1$ changes by unity. This means that $Q$ is much less sensitive to $w_1$ than to $w_0$. It is going to be significantly more difficult to determine a value for $w_1$ from observations of $Q$ (such as supernova observations) in the near future. Comparison of the two cases $z = 1$ and 3 again shows that the sensitivity is somewhat better at high redshifts, but only marginally.

In the above analysis, we have treated $\Omega_m$ as a constant. The situation is made worse by the fact that $Q$ also depends on $\Omega_m$. If the variation of $\Omega_m$ mimics that of $w_0$ or $w_1$, then one also needs to determine the sensitivity of $Q$ to $\Omega_m$. Fig. 10 shows contours of constant $Q$ in the $\Omega_m$–$w_1$ (top frames) and the $\Omega_m$–$w_0$ (bottom frames) planes at two redshifts $z = 1$ (left-hand frames) and $z = 3$ (right-hand frames). The two top frames show that if one varies the value of $\Omega_m$ in the allowed range, say (0.2–0.4), one can move along the curve of constant $Q$ and induce a fairly large variation ($\sim$1–2) in $w_1$. In other words, large changes in $w_1$ can be easily compensated by small changes in $\Omega_m$ while maintaining the same value for $Q$ at a given redshift. This shows that the uncertainty in $\Omega_m$ introduces further difficulties in determining $w_1$ accurately from measurements of $Q$. The two bottom frames show that the situation is better for $w_0$. The curves are much less steep and hence varying $\Omega_m$ does not induce large variations in $w_0$. We once again are led to the conclusion that an unambiguous determination of $w_1$ from data will be quite difficult. It appears that supernova observations

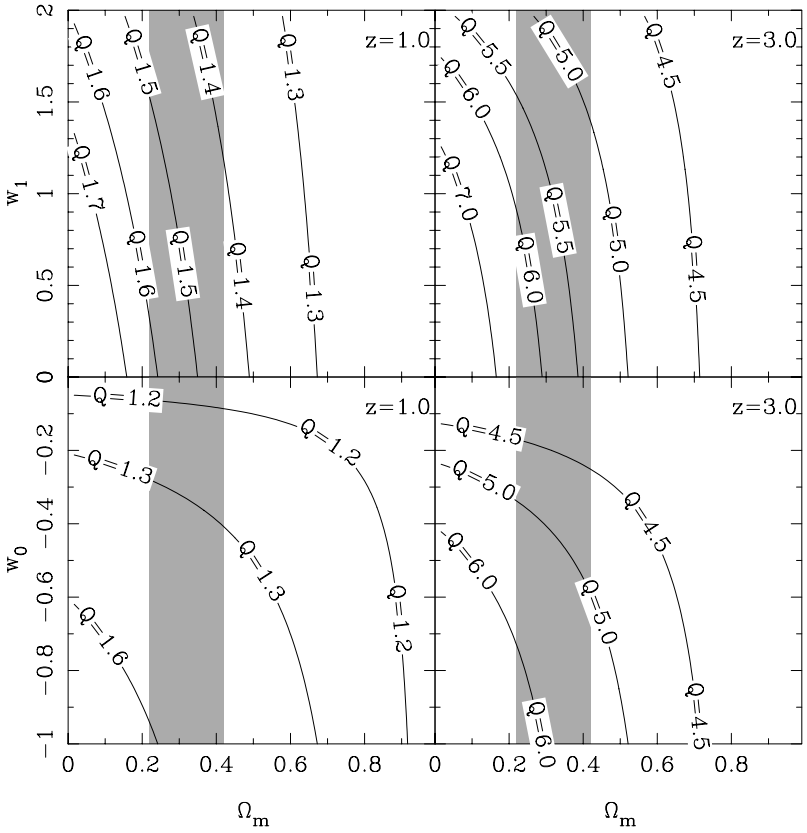


**Figure 10.** Contours of constant $Q$ in the $\Omega_m$–$w_0$ (bottom frames) and $\Omega_m$–$w_1$ (top frames) planes at two redshifts $z = 1$ (left-hand frames) and $z = 3$ (right-hand frames). The value of $w_0$ is fixed to $-1$ in the top frames, while $w_1$ is fixed to 0 in the bottom frames. This figure is available in colour in the online version of the journal on *Synergy*.

may not be of great help in ruling out a (non-evolving) cosmological constant as the major dark energy component.

## 5 DISCUSSION

The supernova data on the whole, rules out non-accelerating models with a very high significance level, as noted and stressed by various authors (Riess et al. 1998; Perlmutter et al. 1999; Riess 2000). It is thus more or less conclusive that we have to look for some form of matter that has negative pressure. However, it is interesting to note that if we divide the data set into high- and low-redshift subsets, neither of the subsets are able to rule out the decelerating models – it is only the interplay between the high- and low-redshift data that implies the result quoted above. This analysis indirectly stresses the importance of any evolutionary effects. Any possible evolution in the absolute magnitude of the supernovae, if detected, might allow the decelerating models to be consistent with the data. However, our understanding of the complicated physical processes in the supernovae is definitely not good enough to discuss the possibility of detecting supernova evolution in the near future. Although the intrinsic evolution of the supernova is an interesting problem, addressing these issues is beyond the scope of this paper.

The supernova data available today is not enough to fix the parameters $\Omega_m$ and $\Omega_\Lambda$ independently. Instead, a particular combination of the two parameters is chosen using the data. This degeneracy has to do with the dependence of the luminosity distance on these parameters. Since supernova observations essentially measure the luminosity distance $Q(z)$, the accuracy in the determination of various parameters from supernova observations will depend crucially on how sensitive $Q$ is to changes in those parameters. This analysis can be done entirely from theory (using the Fisher information matrix; see, for example, Efstathiou 1999) and, in principle, can provide a nice handle on which combinations of parameters are expected to be constrained from the supernova data.

The key issue regarding dark energy is whether it is a constant or whether it is evolving with time. In particular, one is interested in determining the evolution of the equation of state, $w_X$ of the dark energy component. To address this question, we have taken a simple phenomenological model for $w_X$ having the form $w_X(a) = w_0 - w_1(a - 1)$. The sensitivity of the luminosity distance (and hence, the supernova data) on $w_0$ and $w_1$ can be measured by the two parameters ($A$ and $B$) introduced in the paper, which are essentially the fractional changes in $Q(z)$ for unit change in $w_0$ and $w_1$, respectively. The parameters $A$ and $B$ can be obtained entirely from theory and the conclusions drawn from them are valid for current as well as future supernova observations. We find that $Q(z)$ is quite sensitive to $w_0$ – hence, one can constrain the current value of $w_X$ quite well. However, $Q(z)$ is comparatively insensitive to $w_1$, thus determining the evolution of $w_X$ will be a difficult task. The situation is further worsened when we take the uncertainties in $\Omega_m$ into account. Our results are consistent with other statistical analyses made by Astier (2000), Maor, Brustein & Steinhardt (2001), Weller & Albrecht (2001), Maor et al. (2002) and Weller & Albrecht (2002). They have shown that it is possible to constrain the present value of $w_X$ with future missions such as '*SuperNovae Acceleration Probe*' (*SNAP*); however, constraining the evolution of $w_X$ will not be easy using *SNAP*, particularly when $\Omega_m$ is not known to a high accuracy.

## ACKNOWLEDGMENT

TRC is supported by the University Grants Commission, India.


## REFERENCES


Astier P., 2000, preprint (astro-ph/0008306)
Bagla J.S., Padmanabhan T., Narlikar J.V., 1996, Comment. Astrophys., 18, 275
Benítez N., Riess A., Nugent P., Dickinson M., Chornock R., Filippenko A.V., 2002, ApJ, 577, L1
Efstathiou G., 1999, MNRAS, 310, 842
Efstathiou G., Sutherland W.J., Maddox S.J., 1990, Nat, 348, 705
Efstathiou G., Bond J.R., White S.D.M., 1992, MNRAS, 258, 1P
Ellis G.F.R., Madsen M.S., 1991, Class. Quantum Grav., 8, 667
Gerke B.F., Efstathiou G., 2002, MNRAS, 335, 33
Goobar A., Perlmutter S., 1995, ApJ, 450, 14
Hamuy M., Phillips M.M., Suntzeff N.B., Schommer R.A., Maza J., Aviles R., 1996, AJ, 112, 2391
Huterer D., Turner M.S., 1999, Phys. Rev. D, 60, 081301
Maor I., Brustein R., Steinhardt P.J., 2001, Phys. Rev. Lett., 86, 6
Maor I., Brustein R., McMahon J., Steinhardt P.J., 2002, Phys. Rev. D, 65, 123003
Padmanabhan T., 2002a, Theoretical Astrophysics, Volume III: Galaxies and Cosmology. Cambridge Univ. Press, Cambridge
Padmanabhan T., 2002b, Phys. Rev. D, 66, 021301
Padmanabhan T., 2003, Phys. Rep., 380, 235
Padmanabhan T., Choudhury T.R., 2002, Phys. Rev. D, 66, 081301
Padmanabhan T., Narasimha D., 1992, MNRAS, 259, 41P
Perlmutter S. et al., 1999, ApJ, 517, 565
Press W.H., Teukolsky S.A., Vetterling W.T., Flannery B.P., 1992, Numerical Recipes in FORTRAN. The Art of Scientific Computing. Cambridge Univ. Press, Cambridge
Riess A.G., 2000, PASP, 112, 1284
Riess A.G. et al., 1998, AJ, 116, 1009
Riess A.G. et al., 2001, ApJ, 560, 49
Sen A., 2002a, J. High Energy Phys., 07, 065
Sen A., 2002b, Mod. Phys. Lett., A, 17, 1797
Sen A., 2002, JHEP, 04, 048
Sievers J.L. et al., 2003, ApJ, 591, 599
Weller J., Albrecht A., 2001, Phys. Rev. Lett., 86, 1939
Weller J., Albrecht A., 2002, Phys. Rev. D, 65, 103512


## APPENDIX A: DATA ANALYSIS

In this section, we shall outline the method used to obtain the best-fitting (theoretical) parameters from observational data, and draw the corresponding confidence contours. For simplicity, we shall assume that the measurement errors are normally distributed. Suppose we have $M$ observational data points denoted by $m_{\rm obs}(z_i)$; $i = 1, \ldots, M$ with corresponding errors $\sigma_m(z_i)$. For a given theoretical model $m_{\rm th}(z; c_\alpha)$ with $\nu$ free parameters $c_\alpha$; $\alpha = 1, \ldots, \nu$, one can construct the quantity

$$\chi^2(c_\alpha) = \sum_{i=1}^{M} \left[ \frac{m_{\rm obs}(z_i) - m_{\rm th}(z_i; c_\alpha)}{\sigma_m(z_i)} \right]^2 . \tag{A1}$$

The best-fitting parameters $\bar{c}_\alpha$ are obtained by minimizing the above quantity

$$\left( \frac{\partial \chi^2}{\partial c_\alpha} \right)_{c_\alpha = \bar{c}_\alpha} = 0 \tag{A2}$$

using the Levenberg–Marquardt method (Press et al. 1992). One can show that the quantity $\Delta\chi^2 = \chi^2(c_\alpha) - \chi^2(\bar{c}_\alpha)$ follows a chi-square distribution with $\nu$ degrees of freedom.

To obtain the confidence intervals, let us first define the curvature matrix

$$A_{\alpha\beta} = \frac{1}{2} \left( \frac{\partial^2 \chi^2}{\partial c_\alpha \partial c_\beta} \right)_{c_\alpha = \bar{c}_\alpha} . \tag{A3}$$

The covariance matrix $C_{\alpha\beta}$ is simply the inverse of the curvature matrix. The probability distribution of the parameters is given by

$$\mathcal{P}(c_\alpha) = \text{constant} \times \exp \left[ -\frac{1}{2} \sum_{\alpha,\beta=1}^{\nu} (c_\alpha - \bar{c}_\alpha) A_{\alpha\beta} (c_\beta - \bar{c}_\beta) \right]. \tag{A4}$$

Suppose we are interested in the confidence regions for a subset of, say, $\nu'$ parameters ($\nu' \leqslant \nu$). In that case, the regions are obtained by simply marginalizing the probability distribution over the rest $\nu - \nu'$ parameters [which is equivalent to integrating the probability distribution (A4) over the rest of the $\nu - \nu'$ parameters]. This can be done simply by taking the full $\nu \times \nu$ covariance matrix $C_{\alpha\beta}$ and copying the intersection of the $\nu'$ rows and columns corresponding to the parameters of interest into a $\nu' \times \nu'$ matrix $C'_{\alpha\beta}$. The inverse of this will give the corresponding curvature matrix $A'_{\alpha\beta}$ (Press et al. 1992). The marginalized probability distribution will be simply

$$\mathcal{P}'(c_\alpha) = \text{constant} \times \exp \left[ -\frac{1}{2} \sum_{\alpha,\beta=1}^{\nu'} (c_\alpha - \bar{c}_\alpha) A'_{\alpha\beta} (c_\beta - \bar{c}_\beta) \right]. \tag{A5}$$

Next, one needs to find the quantity $\Delta\chi^2_p$, such that the probability of a chi-square variable with $\nu'$ degrees of freedom being less than $\Delta\chi^2_p$ is $p$, where $p$ is the desired confidence limit (e.g. 0.68 or 0.95). This can be obtained by solving the equation

$$p = \frac{1}{2^{\nu'/2}\Gamma(\nu'/2)} \int_0^{\Delta\chi^2_p} {\rm d}u\, u^{(\nu'/2)-1} {\rm e}^{-u/2}, \tag{A6}$$

where $\Gamma(z)$ is the gamma function. For a given $p$ and a set of $\nu'$ parameters, the equation for the boundary of the confidence region in the $\nu'$-dimensional space is given by the equation

$$\Delta\chi^2_p = \sum_{\alpha,\beta=1}^{\nu'} (c_\alpha - \bar{c}_\alpha) A'_{\alpha\beta} (c_\beta - \bar{c}_\beta). \tag{A7}$$

## APPENDIX B: DETERMINATION OF THE HUBBLE PARAMETER $H(z)$ FROM SUPERNOVA OBSERVATIONS

The observational data used in this paper can be fitted by the function of simple form

$$m_{\rm fit}(z) = a_1 + 5 \log_{10} \left[ \frac{z(1 + a_2 z)}{1 + a_3 z} \right], \tag{B1}$$

where the parameters are

$$a_1 = 23.95 \pm 0.05; \quad a_2 = 2.00 \pm 1.18; \quad a_3 = 1.03 \pm 0.88. \tag{B2}$$

The $\chi^2$ per degree of freedom for the best-fitting values of the parameters is found to be 1.05, which shows the fit is reasonably good. The difference between the data points and the fit is shown in Fig. B1. We can then represent the luminosity distance obtained from the data by the function

$$Q_{\rm fit}(z) = 10^{0.2[m_{\rm fit}(z) - \mathcal{M}]}. \tag{B3}$$

Note that one needs to fix the value of $\mathcal{M}$ to obtain the function $Q_{\rm fit}(z)$. For flat models, the value of $\mathcal{M}$ is well constrained (the

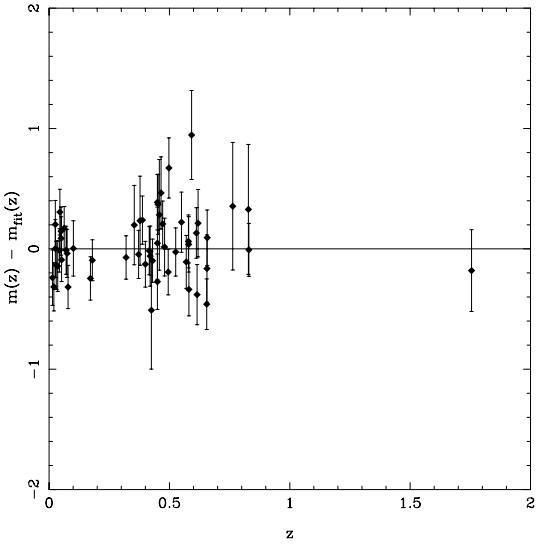


**Figure B1.** The difference between the actual data points and the fit (B1) to the data.

error being ∼1 per cent) – hence we can use the best-fitting value of $\mathcal{M} = 23.95$ to obtain

$$Q_{\rm fit}(z) = \frac{z(1+2.00z)}{1+1.03z}. \tag{B4}$$

For flat models, it straightforward to obtain the Hubble parameter from $Q(z)$. In particular, we are interested in the quantity

$$H_0^{-1}\dot{a}(z) = \left\{(1+z)\frac{\rm d}{{\rm d}z}\left[\frac{Q(z)}{1+z}\right]\right\}^{-1}, \tag{B5}$$

which will enable us to plot the data points in the $\dot{a} - a$ plane. The determination of the corresponding error bars is a non-trivial exercise. In this paper, the errors are obtained from the relation

$$H_0^{-1}\dot{a}(z)[1+\epsilon_{\dot{a}}(z)] = \left[(1+z)\frac{\rm d}{{\rm d}z}\left\{\frac{Q(z)[1+\epsilon_Q(z)]}{1+z}\right\}\right]^{-1}, \tag{B6}$$

where $\epsilon_{\dot{a}}$ and $\epsilon_Q$ denote the fractional error in $\dot{a}$ and $Q$, respectively. From equation (18), we have $\epsilon_Q(z) = 0.2 \ln 10\, \sigma_m(z)$, where $\sigma_m(z)$ is the total uncertainty in the observed magnitude. Since there is no systematic evolution of the observed $\sigma_m(z)$ (see Fig. B1), we have, to the lowest approximation, the fractional error in $\dot{a}$

$$\epsilon_{\dot{a}}(z) = \epsilon_Q(z) = 0.2(\ln 10)\,\sigma_m(z). \tag{B7}$$

Thus, one can plot the quantity $\dot{a}(z)$ for the observational data with error bars given by the above equation.

Note that the analysis assumes that the observed errors in the measurement of $z$ (or, equivalently $a$) are negligible. Strictly speaking, the errors in $\dot{a}$ calculated above are strict lower limits – they can be slightly higher because of the errors arising from (i) the fitting function and (ii) any systematic evolution of the observed $\sigma_m(z)$. However, these effects are unlikely to affect any of the conclusions we have drawn in this paper.

This paper has been typeset from a TEX/LATEX file prepared by the author.